Cobalt-ferrite nanobowl arrays : curved magnetic nanostructures

Srivastava, A. K.; Madhavi, S.; Ramanujan, R. V.; White, Timothy John

2007

Cobalt–ferrite nanobowl arrays: Curved magnetic nanostructures

A.K. Srivastava, S. Madhavi, T.J. White, and R.V. Ramanujan[a]
School of Materials Science and Engineering, Nanyang Technological University, Singapore 639798

Novel magnetic cobalt ferrite nanostructures with curved surfaces (i.e., nanobowls and hollow nanospheres) in a periodic array have been fabricated by in situ reduction of a cobalt and iron salt solution mixture in the interstitial spaces of three-dimensional, close-packed, polystyrene sphere templates. The effect of the shape created by this nanostructure and magnetocrystalline anisotropy introduced by suitable annealing were used to tailor the coercivity to values relevant to high-density data-storage applications.

I. INTRODUCTION

Nanostructured magnetic materials[1–6] are of tremendous interest due to their relevance in high-density data-storage devices[5–8] and biomedical applications.[9] Recently, curved magnetic nanostructures have been shown to control magnetization reversal, thus making them relevant to data-storage applications.[8,9] One of the other emerging applications of magnetic nanobowls is in the area of drug delivery; the bowls can be loaded with drugs that are targeted to the disease site via an external magnetic field. Magnetic nanostructures of cobalt (Co),[5,6] nickel (Ni),[5,10] iron (Fe),[5] nickel–iron (Ni–Fe),[5] and iron–platinum (Fe–Pt)[11] with curved shapes, known variously as macroporous, nanobowls, or hollow spheres, exhibit enhanced coercivities in comparison to their bulk, thin-film, or nanoparticle counterparts. Individual nano-elements of similar shapes can be produced using template-free hydrothermal synthesis[10,12]; however, ordered structure is essential to achieving high-density data-storage applications. High coercivity is useful in such applications to prevent information being erased by the stray field in the network; on the other hand, too high a value can make it difficult to write information. It has been suggested that arrays of data elements with coercivities between 500 and 1000 Oersted (Oe) are most suitable in the context of perpendicular recording media.[13]

A number of techniques are available to reduce the particle size of ferromagnetic materials as well as to arrange them in periodic arrays. Colloidal crystal templating[5,6,10,14–17] is a low-cost and rapid technique for the assembly of nanobowl and hollow-sphere magnetic networks. Electrodeposition[5,15,16] and the chemical conversion of precursors[6,16,17] in the interstitial spaces of such templates have been widely used to create such nanostructures. Ferrite nanoparticles are of interest due to their useful magnetic properties, and many groups have reported the synthesis of cobalt ferrite nanoparticles[18–20] and nanowires,[21] but the fabrication of cobalt ferrite nanostructures with curved surfaces has received much less attention. Recent work discussing the suitability of magnetic nanostructures with curved surfaces[7,8] has created interest in the synthesis of cobalt ferrite nanobowls.

In this article, we report on the fabrication of a novel nanostructure of cobalt ferrite called a "nanobowl" in a three-dimensional periodic array by employing self-assembled colloidal polymer spheres as templates. By controlling the shape and magnetocrystalline anisotropy, we have succeeded in achieving an ordered array of magnetic nanobowls with coercivity values in the range of 500 to 1000 Oe. The morphology of these multilayered nanostructures, which was studied using electron microscopy, revealed nanobowls and hollow-sphere networks of cobalt ferrite. Earlier reports on ferromagnetic nanostructured materials focused on the morphology of the top layer rather than the underlayers.[5,6,11] Our observations show that bowls in the underlayers of the network have a shape that is very similar to that of hollow spheres. Based on this, we propose a mechanism for the formation of such curved nanostructures. The structural properties of these nanostructures have been investigated using a powder x-ray diffraction (XRD) technique. Further, the effect of shape and crystal structure on the magnetic properties of nanobowl arrays is presented and discussed.

II. EXPERIMENTAL PROCEDURES

To synthesize nanobowl structures, 0.3 M cobalt chloride $CoCl_2$–$6H_2O$ (APS Ajax Finechem, Australia), 0.3 M iron chloride $FeCl_2$–$4H_2O$ (Merck KGaA, Germany),

and 0.6 M sodium borohydride $NaBH_4$ (Fluka, Milwaukee, WI) solutions were prepared in deionized water. First, the solution mixture of $CoCl_2$–$6H_2O$ and $FeCl_2$–$4H_2O$ was vacuum-impregnated inside interstitials of close-packed polystyrene (PS) templates prepared from the centrifugation of 1-μm PS spheres. This was followed by the addition of sodium borohydride $NaBH_4$; the ensuing reaction leads to the formation of nanoparticles in the interstitial spaces of the template. The infiltrated template was dried for 24 h, and the infiltration process was repeated to ensure the complete filling of the interstitial spaces by the particles. These steps were performed inside a N_2-filled dry box (Plas Laboratories, Lansing, MI). Template removal was carried out either by toluene etching or by annealing the sample at 400 or 500 °C for 4 h in air followed by toluene etching. Nanoparticles were synthesized by mixing the solution mixture of cobalt and iron salts and sodium borohydride as described without using the PS template.

The morphology of the nanobowl arrays was investigated using a field-emission scanning electron microscope (JSM-6340F, JEOL, Japan). Transmission electron microscopy (TEM) (JEM-2010; JEOL, Tokyo, Japan) was used to analyze the nanoparticles. Powder XRD patterns of the nanobowl samples were collected using a Shimadzu (Japan) 6000 Lab X diffractometer with Cu K$_\alpha$ radiation using step scans in the 2θ range of 20–80°. Magnetic measurements were carried out at room temperature using a Lakeshore (Westerville, OH) 7404 vibrating sample magnetometer.

III. RESULTS AND DISCUSSION

Secondary electron images of the cobalt–ferrite nanobowl arrays are shown in Fig. 1. Removal of the PS template was achieved either by etching with toluene or by annealing. The topmost layer of the as-synthesized sample [Fig. 1(a)], for which the template was removed by toluene etching, exhibits a bowl-like morphology with shell thicknesses in the sub-100-nm regime. The discontinuous formation of material can be observed within the interstitials in accordance with our earlier work on cobalt nanobowls.[6] The dark regions seen in Fig. 1(a) are the interconnections within the network, arising from the points of contact of the PS spheres. The precursor infiltration did not occur at these points of contact. Figures 1(b) and 1(c) present the morphology of the samples for which template removal was carried out by annealing at 400 °C for 4 h followed by toluene etching. The top layer of the structure exhibits nanobowl formation [Fig. 1(b)]. On the other hand, the morphology of the underlayers resembles that of hollow spheres [Fig. 1(c)]. The hollow nature of these spheres has been confirmed by the broken spheres [shown in the inset of Fig. 1(c)]. Previous investigations of such nanobowls or macroporous materials have highlighted the bowl shape of the top layer, but the hollow spherical morphology of underlayers was not highlighted.[5,6,11] When the sample is annealed at 500 °C for 4 h in air, the periodicity of the array was disrupted by diffusional processes, which led to growth and coarsening [Fig. 1(d)].
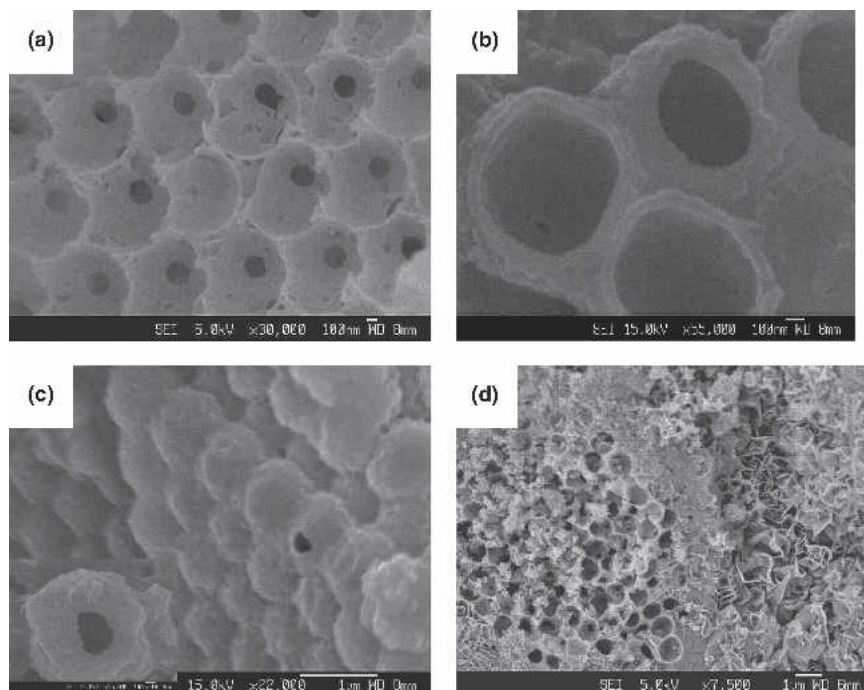

FIG. 1. Morphology of nanobowl samples (a) as-synthesized, (b) annealed at 400 °C for 4 h (top layer), (c) annealed at 400 °C for 4 h (underlayers), and (d) annealed at 500 °C for 4 h.
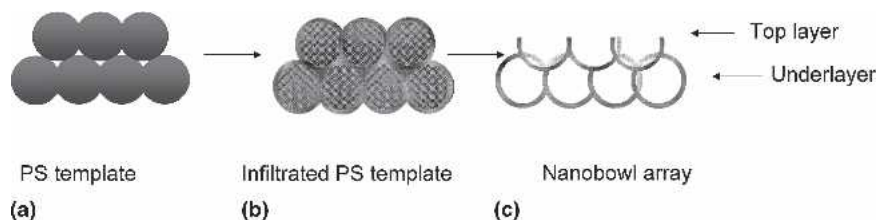
FIG. 2. Schematic for the formation of nanobowls and hollow spheres.

Figure 2 presents the schematic leading to the formation of two different curved morphologies (compared to the nanobowl and hollow sphere). Figure 2(a) shows an ordered close-packed PS sphere template. Nanoparticles are formed by in situ reduction inside the interstitial voids in between the PS spheres and thus acquire the shape of the spheres [Fig. 2(b)]. Vacuum suction was applied to infiltrate the precursors into the underlayers, which leads to the formation of thicker layers of nanoparticles in the underlayers compared to the top layer. When an etching sequence is applied to remove the PS spheres, unlike the underlayers, which are supported by the upper layers in the network, the topmost layer adopts a bowl-shaped morphology instead of the hollow-sphere morphology. Removal of the PS spheres from the underlayers resulted in a hollow-sphere morphology [Fig. 2(c)]. The thicknesses of the nanobowls in the top layer is less than the diameter of the PS spheres, while the thicknesses of the hollow spheres in the underlayers are equal to the diameter of the PS spheres used in the template. The formation of hollow spheres can also occur due to the overinfiltration of precursors, also leading to the formation of hollow-sphere morphology in the top layer,

as observed previously in the case of the synthesis of cobalt and cobalt oxide hollow spheres.[22]

Nanoparticles were also synthesized by borohydride reduction of the same solution mixture of cobalt and iron salts as that used for the nanobowl array without using templates. Figure 3 shows the TEM micrograph of the polydisperse nanoparticles in the size range 5–45 nm. The XRD patterns of the samples presented in Fig. 4 show the effect of the annealing temperature on crystallinity. The as-synthesized nanobowl sample, for which the template removal was carried out only by toluene etching, is amorphous [Fig. 4(a)]. Annealing results in crystallization; the major peak observed for samples annealed at 400 °C for 4 h [Fig. 4(b)] was the (311) plane of a cubic unit cell of a spinel $CoFe_2O_4$ structure, while the peaks observed for samples annealed at 500 °C for 4 h [Fig. 4(c)] can be indexed as (200), (311), (400), (422), (511), (440), and (622) planes (JCPDS Card No. 22-1086). However, energy-dispersive x-ray spectroscopy (EDS) results for the sample annealed at 400 °C show that the atomic percentages of Co, Fe, and O are 25, 25, and 50 at.%, respectively (Co/Fe ratio ≈ 1:1), which is the same as the Co/Fe ratio in the precursor, consistent with the value (0.81) reported by Li et al.[23] for 1:1 molar ratio of Co/Fe in precursor solution. Li et al.[23] also observed the spinel cobalt ferrite structure for a 1:1 molar
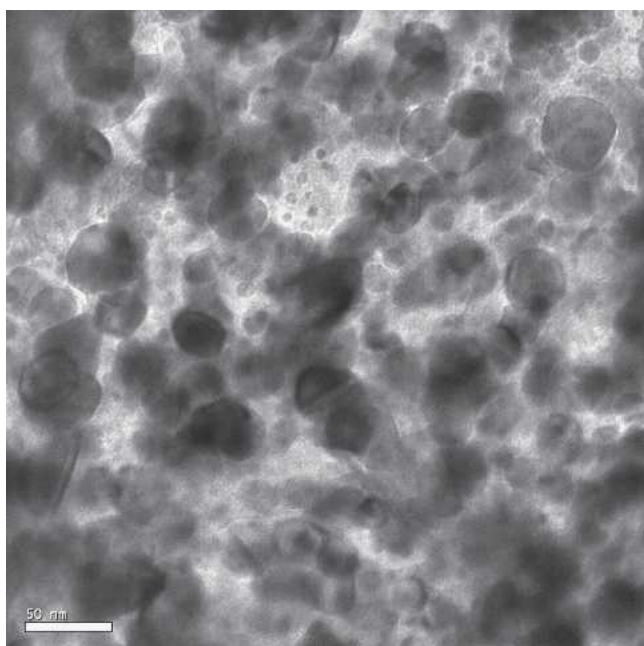

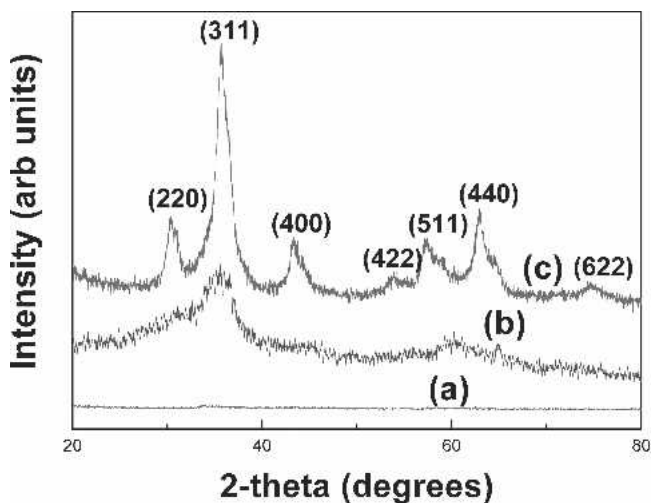FIG. 3. TEM micrograph of the as-synthesized nanoparticles.

FIG. 4. XRD pattern of the nanobowl samples (a) as-synthesized, (b) annealed at 400 °C for 4 h, and (c) 500 °C for 4 h.
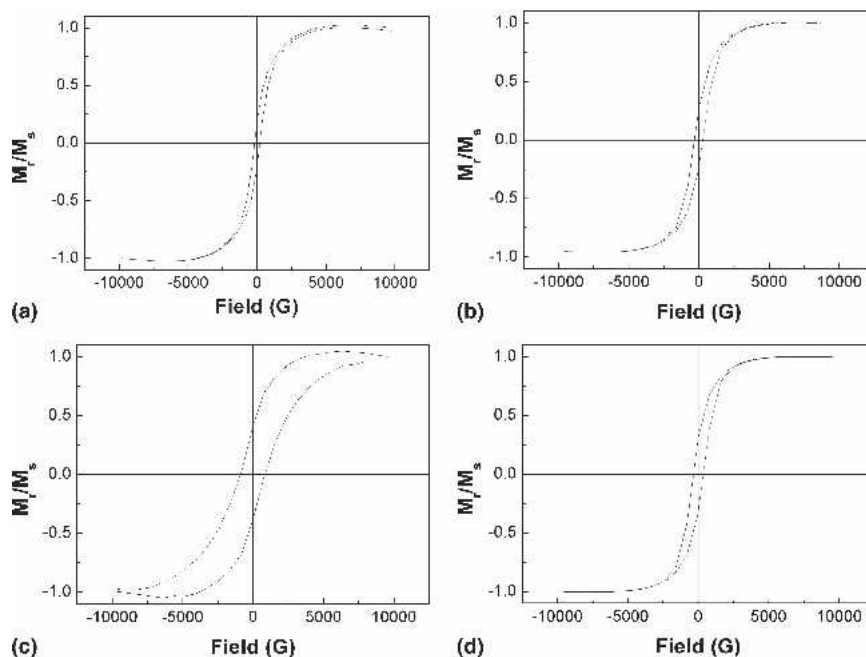
FIG. 5. Magnetization curves for (a) as-synthesized nanoparticles, (b) as-synthesized nanobowls, and cobalt–ferrite nanobowls annealed at (c) 400 °C for 4 h and (d) 500 °C for 4 h.

ratio of Co/Fe in precursor solution, which is in agreement with our result. The EDS results for the sample annealed at 500 °C (Co 25 at.%; Fe 25 at.%; and O 50 at.%) show that the 1:1 atomic ratio of Co/Fe was retained.

The magnetic properties were also investigated. The coercivity of the as-synthesized nanobowl array, for which the template removal was carried out by toluene etching, was found to be 299.0 Oe (23.8 kA/m) [Fig. 5(a)]. To examine the effect of shape on the magnetic properties, the magnetic properties of the nanoparticles were measured. These nanoparticles exhibit coercivity of 215.9 Oe (17.1 kA/m) [Fig. 5(b)], which indicates that the nanobowl array has ~39% higher coercivity compared to the nanoparticles. Recently, a difference in coercivity (~26%) of such morphologies of nickel has been reported.[24] The squareness value of the as-synthesized nanobowls array (0.26) was also found to be greater than the squareness of the as-synthesized nanoparticles (0.16). The induced shape effect of the bowl plays an important role in increasing the coercivity. Because nanoparticles of <10 nm in size were also observed in the TEM micrograph presented in Fig. 3, the magnetic properties of such small particles will be affected by thermal excitations (i.e., the superparamagnetic limit) and will lead to low coercivity,[18] but when particles are synthesized in the interstitials of a template, they form aggregates in the shape of larger-sized walls of bowls. Hence, they are unaffected by thermal excitations, which leads to higher coercivity value. The enhancement in coercivity can also be explained in terms of domain-wall motion. Domain-

wall pinning due to the network structure and the shell of nanobowls or hollow spheres can lead to higher coercivity.[25] The shell structure is composed of nanoparticles and hence can be considered as a rough surface, this roughness can also cause domain-wall pinning. The coercivity is dependent on domain-wall motion and because the barrier to domain-wall propagation along a curved surface is greater than that of a flat surface[26]; curved surfaces show a high coercivity value. According to Skomski,[27] the coercivity is inversely proportional to the square of the domain-wall curvature and hence can be expected to be high for curved surfaces. Such an increase in coercivity compared to those of nanoparticles and thin-film morphologies or bulk material has also been observed in previous reports.[5,6,10,11]

In addition to shape effects, important magnetocrystalline anisotropy effects were also observed. The coercivity of the sample annealed at 400 °C for 3 h was 862.8 Oe (68.7 kA/m) [Fig. 5(c)], which was much greater than that for the as-synthesized sample (299.0 Oe). The coercivity of the sample annealed at 500 °C was found to have a coercivity of 349.0 Oe (27.8 kA/m) [Fig. 5(d)], which is lower than the sample annealed at 400 °C. The squareness value of the sample annealed at 400 °C (0.38) was also found to be higher than that of the sample annealed at 500 °C (0.31). The increase in coercivity can be explained in terms of magnetocrystalline anisotropy; the sample annealed at 400 °C reveals uniaxial anisotropy, because the strongest XRD peak was observed for the (311) plane [i.e., it exhibits preferred orientation along (311) planes]. On the other hand, when the sample

is annealed at 500 °C it exhibits cubic anisotropy with multiple easy axes leading to a decrease in coercivity. The broken-bowl structure may be an additional factor influencing the coercivity.

IV. CONCLUSION

In summary, cobalt ferrite nanobowl arrays were chemically synthesized by the borohydride reduction of a solution mixture of cobalt and iron salts using a colloidal–crystal-templating technique. The morphology of the underlayers is that of an ordered array of hollow spheres in contrast to that of the top layer, which is bowl-shaped. An enhancement in the coercivity value of nanobowls in comparison to that of nanoparticles was observed due to shape effects. The crystallinity was altered by suitable annealing; thus, the magnetocrystalline anisotropy and the coercivity value could be controlled. Optimum properties were achieved for nanobowl arrays annealed at 400 °C.

REFERENCES

1. M.A. Willard, L.K. Kurihara, E.E. Carpenter, S. Calvin, and V.G. Harris: Chemically prepared magnetic nanoparticles. *Inter. Mater. Rev.* **49,** 125 (2004).
2. T. Hyeon: Chemical synthesis of magnetic nanoparticles. *Chem. Commun.* 927 (2003)
3. C-M. Liu, L. Guo, R-M. Wang, Y. Deng, H-B. Xu, and S. Yang: Magnetic nanochains of metal formed by assembly of small nanoparticles. *Chem. Commun.* 2726 (2004).
4. V.F. Puntes, K.M. Krishnan, and P. Alivisatos: Colloidal nanocrystal shape and size control: The case of cobalt. *Science* **291,** 2115 (2001).
5. P.N. Bartlett, M.A. Ghanem, I.S.E. Hallag, P.D. Groot, and A. Zhukov: Electrochemical deposition of macroporous magnetic networks using colloidal templates. *J. Mater. Chem.* **13,** 2596 (2003).
6. A.K. Srivastava, S. Madhavi, T.J. White, and R.V. Ramanujan: Template assisted assembly of cobalt nanobowl arrays. *J. Mater. Chem.* **15,** 4424 (2005).
7. T.C. Ulbrich, D. Makarov, G. Hu, I.L. Guhr, D. Suess, T. Schrefl, and M. Albrecht: Magnetization reversal in a novel gradient nanomaterial. *Phys. Rev. Lett.* **96,** 077202 (2006).
8. M. Albrecht, G. Hu, I.L. Guhr, T.C. Ulbrich, J. Boneberg, P. Leiderer, and G. Schatz: Magnetic multilayers on nanospheres. *Nat. Mater.* **4,** 203 (2005).
9. C.C. Berry: Possible exploitation of magnetic nanoparticles: Cell interaction for biomedical applications. *J. Mater. Chem.* **15,** 543 (2005).
10. Q. Liu, H. Liu, M. Han, J. Zhu, Y. Liang, Z. Xu, and Y. Song: Nanometer-sized nickel hollow spheres. *Adv. Mater.* **17,** 1995 (2005).
11. F. Iskandar, T. Iwaki, T. Toda, and K. Okuyama: High coercivity of ordered macroporous FePt films synthesized via colloidal templates. *Nano Lett.* **5,** 1525 (2005).
12. Y. Wang, Q. Zhu, and H. Zhang: Fabrication of β-Ni(OH)$_2$ and NiO hollow spheres by a facile template-free process. *Chem. Commun.* 5231 (2005).
13. H. Daimon, O. Kitakami, O. Inagoya, and A. Sakemoto: Magnetic properties of Fe-Cu and Fe-P electrodeposited alumite films. *Jpn. J. Appl. Phys.* **30,** 282 (1991).
14. A.A. Zhukov, A.V. Goncharov, P.A.J. de Groot, P.N. Bartlett, and M.A. Ghanem: Magnetic antidot arrays from self-assembly template methods. *J. Appl. Phys.* **93,** 7322 (2003).
15. P.N. Bartlett, P.R. Birkin, and M.A. Ghanem: Electrochemical deposition of macroporous platinum, palladium and cobalt films using polystyrene latex sphere templates. *Chem. Commun.* 1671 (2000).
16. H. Yan, C.F. Blanford, W.H. Smyrl, and A. Stein: Preparation and structure of 3D ordered macroporous alloys by PMMA colloidal crystal templating. *Chem. Commun.* 1477 (2000).
17. A.K. Srivastava, S. Madhavi, T.J. White, and R.V. Ramanujan: The processing and characterization of magnetic nanobowls. *Thin Solid Films* **505,** 93 (2006).
18. S. Bhattacharyya, J-P. Salvetat, R. Fleurier, A. Husmann, T. Cacciaguerra, and M-L. Saboungi: One step synthesis of highly crystalline and high coercive cobalt-ferrite nanocrystals. *Chem. Commun.* 4818 (2005).
19. Q. Song and Z.J. Zhang: Shape control and associated magnetic properties of spinel cobalt ferrite nanocrystals. *J. Am. Chem. Soc.* **126,** 6164 (2004).
20. S. Li, V.T. John, C. O'Connor, V. Harris, and E. Carpenter: Cobalt-ferrite nanoparticles: Structure, cation distributions, and magnetic properties. *J. Appl. Phys.* **87,** 6223 (2000).
21. J-S. Jung, J-H. Lim, K-H. Choi, S-L. Oh, Y-R. Kim, S-H. Lee, D.A. Smith, K.L. Stokes, L. Malkinski, and C.J. O'Connor: CoFe$_2$O$_4$ nanostructures with high coercivity. *J. Appl. Phys.* **97,** 10F306 (2005).
22. H. Yoshikawa, K. Hayashida, Y. Kozuka, A. Horiguchi, K. Awaga, S. Bandow, and S. Iijima: Preparation and magnetic properties of hollow nano-spheres of cobalt and cobalt oxide: Drastic cooling-field effects on remnant magnetization of antiferromagnet. *Appl. Phys. Lett.* **85,** 5287 (2004).
23. S. Li, L. Liu, V.T. John, C.J. O'Connor, and V.G. Harris: Cobalt–ferrite nanoparticles: correlations between synthesis procedures, structural characteristics and magnetic properties. *IEEE Trans. Magn.* **37,** 2350 (2001).
24. Y. Wang, Q. Zhu, and H. Zhang: Fabrication and magnetic properties of hierarchical porous hollow nickel microspheres. *J. Mater. Chem.* **16,** 1212 (2006).
25. G. Duan, W. Cai, Y. Li, Z. Li, B. Cao, and Y. Luo: Transferable ordered Ni hollow sphere arrays induced by electrodeposition on colloidal monolayer. *J. Phys. Chem. B* **110,** 7184 (2006).
26. S.P. Li, W.S. Lew, Y.B. Xu, A. Hirohata, A. Samad, F. Baker, and J.A.C. Bland: Magnetic nanoscale dots on colloid crystal surfaces. *Appl. Phys. Lett.* **76,** 748 (2000).
27. R. Skomski: Domain-wall curvature and coercivity in pinning type Sm–Co magnets. *J. Appl. Phys.* **81,** 5627 (1997).